Lecture-4
16.484/16.581
Frequency domain analysis summary (cont.)
Spring 2019

Summary

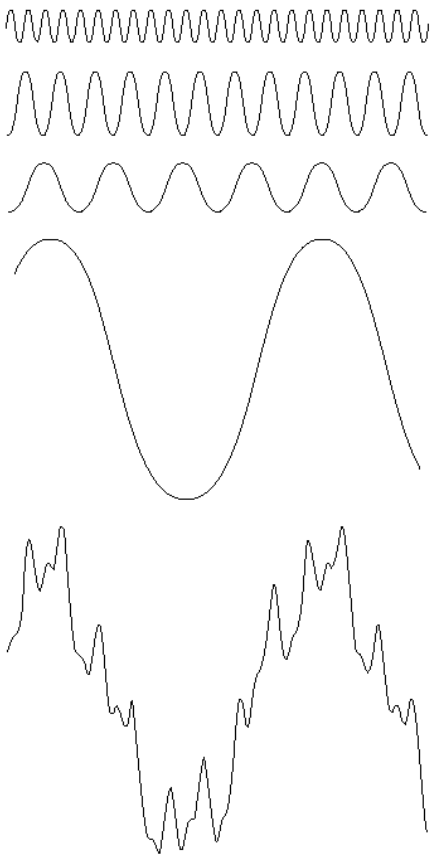

FIGURE 4.1 The function at the bottom is the sum of the four functions above it. Fourier's idea in 1807 that periodic functions could be represented as a weighted sum of sines and cosines was met with skepticism.

Cont.

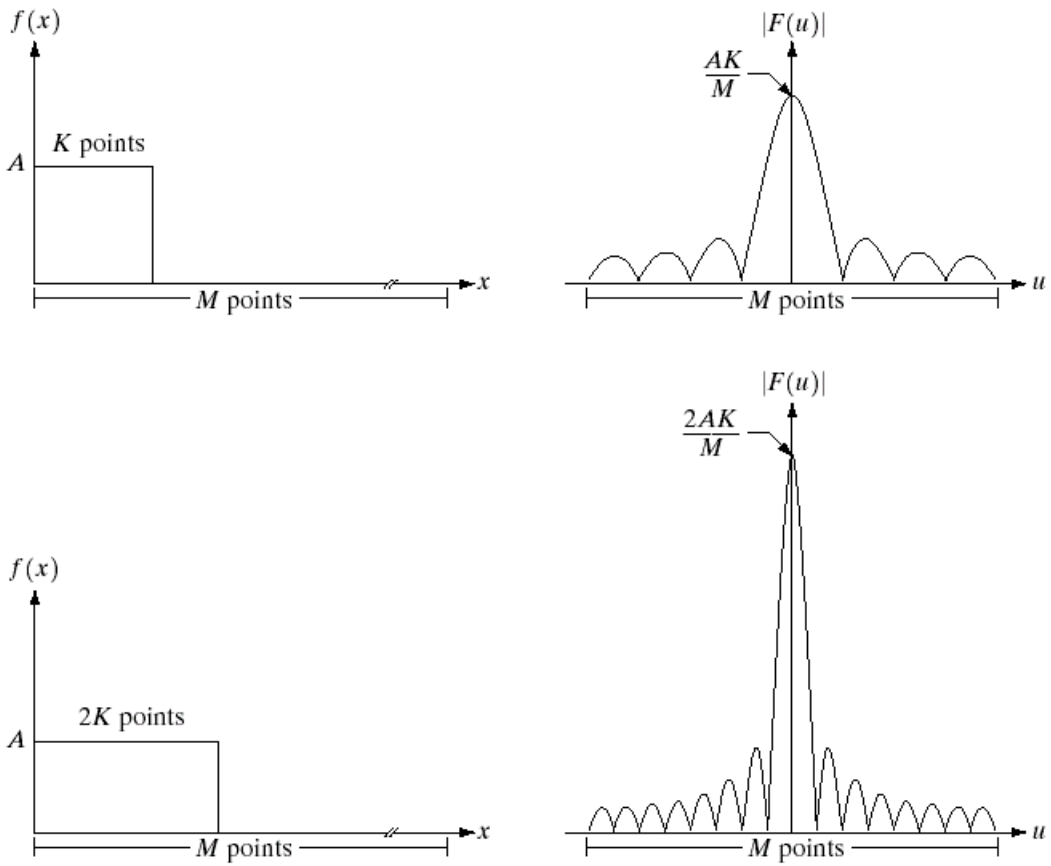

a b
c d

FIGURE 4.2 (a) A discrete function of M points, and (b) its Fourier spectrum. (c) A discrete function with twice the number of nonzero points, and (d) its Fourier spectrum.

Cont.

a b

FIGURE 4.3
(a) Image of a 20×40 white rectangle on a black background of size 512×512 pixels.
(b) Centered Fourier spectrum shown after application of the log transformation given in Eq. (3.2-2). Compare with Fig. 4.2.

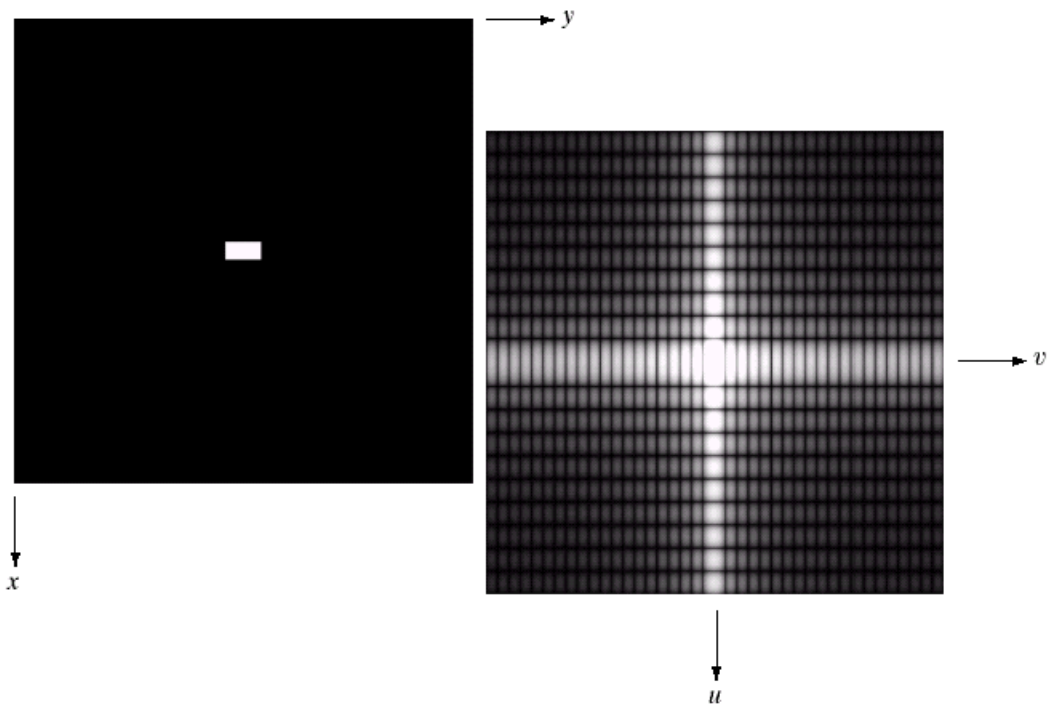

Cont.

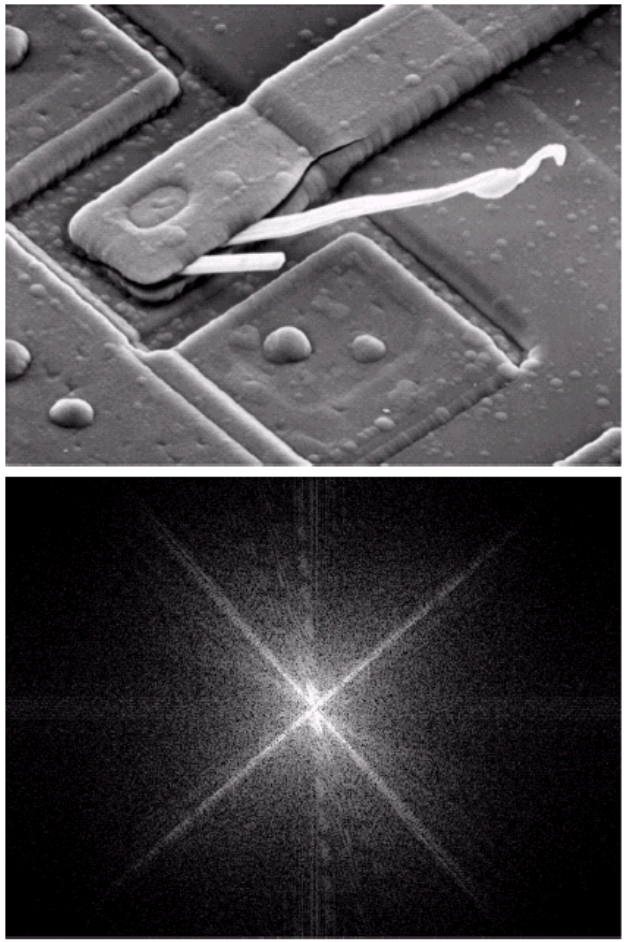

a
b

FIGURE 4.4
(a) SEM image of a damaged integrated circuit. (b) Fourier spectrum of (a). (Original image courtesy of Dr. J. M. Hudak, Brockhouse Institute for Materials Research, McMaster University, Hamilton, Ontario, Canada.)

Cont.

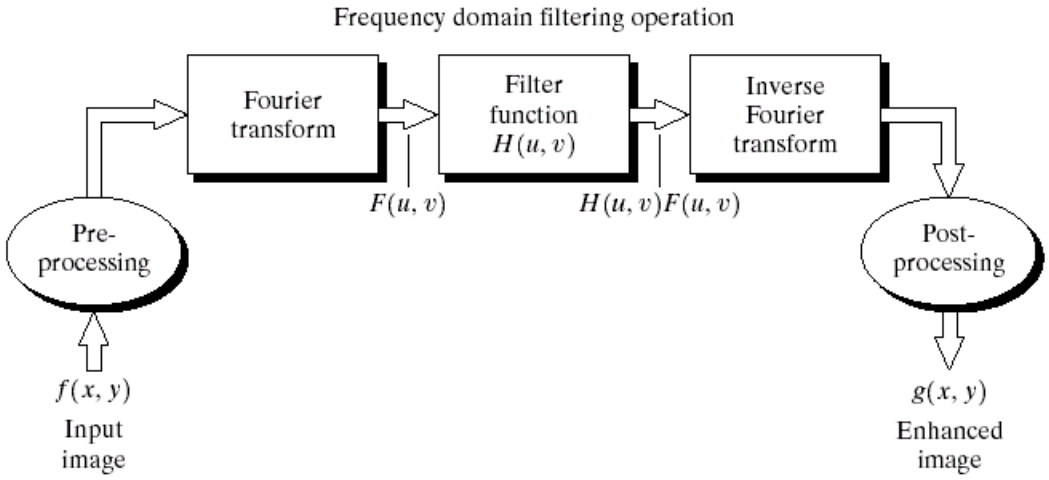

FIGURE 4.5 Basic steps for filtering in the frequency domain.

cont

FIGURE 4.6
Result of filtering the image in Fig. 4.4(a) with a notch filter that set to 0 the $F(0, 0)$ term in the Fourier transform.

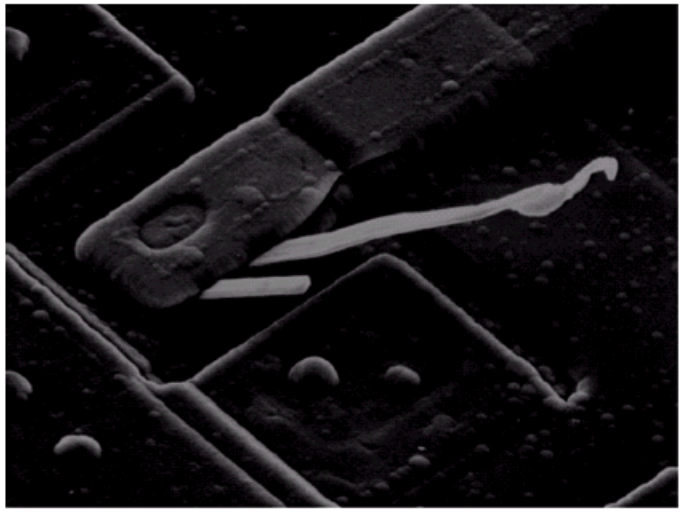

Cont

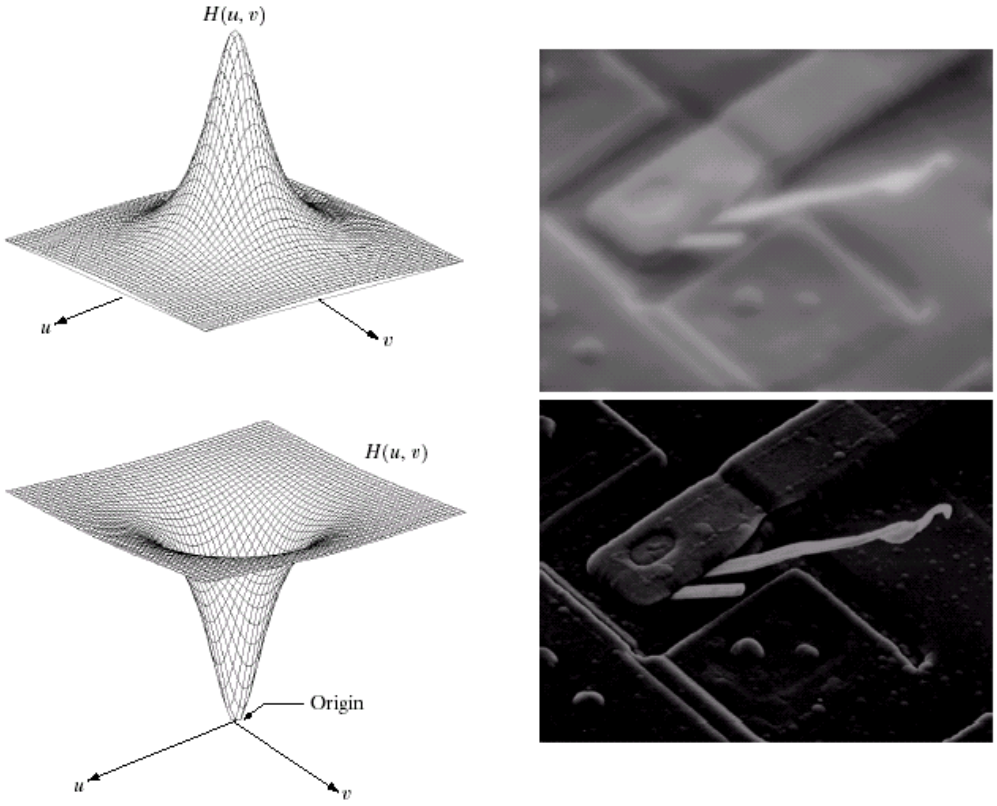

a b
c d

FIGURE 4.7 (a) A two-dimensional lowpass filter function. (b) Result of lowpass filtering the image in Fig. 4.4(a). (c) A two-dimensional highpass filter function. (d) Result of highpass filtering the image in Fig. 4.4(a).

Cont.

FIGURE 4.8
Result of highpass filtering the image in Fig. 4.4(a) with the filter in Fig. 4.7(c), modified by adding a constant of one-half the filter height to the filter function. Compare with Fig. 4.4(a).

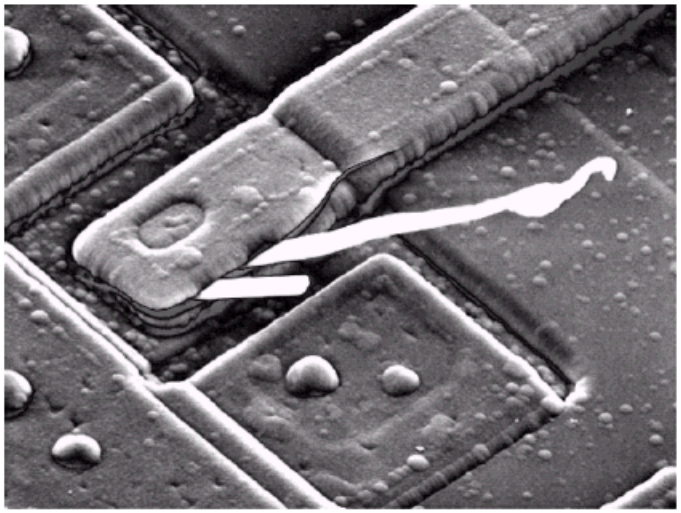

Cont

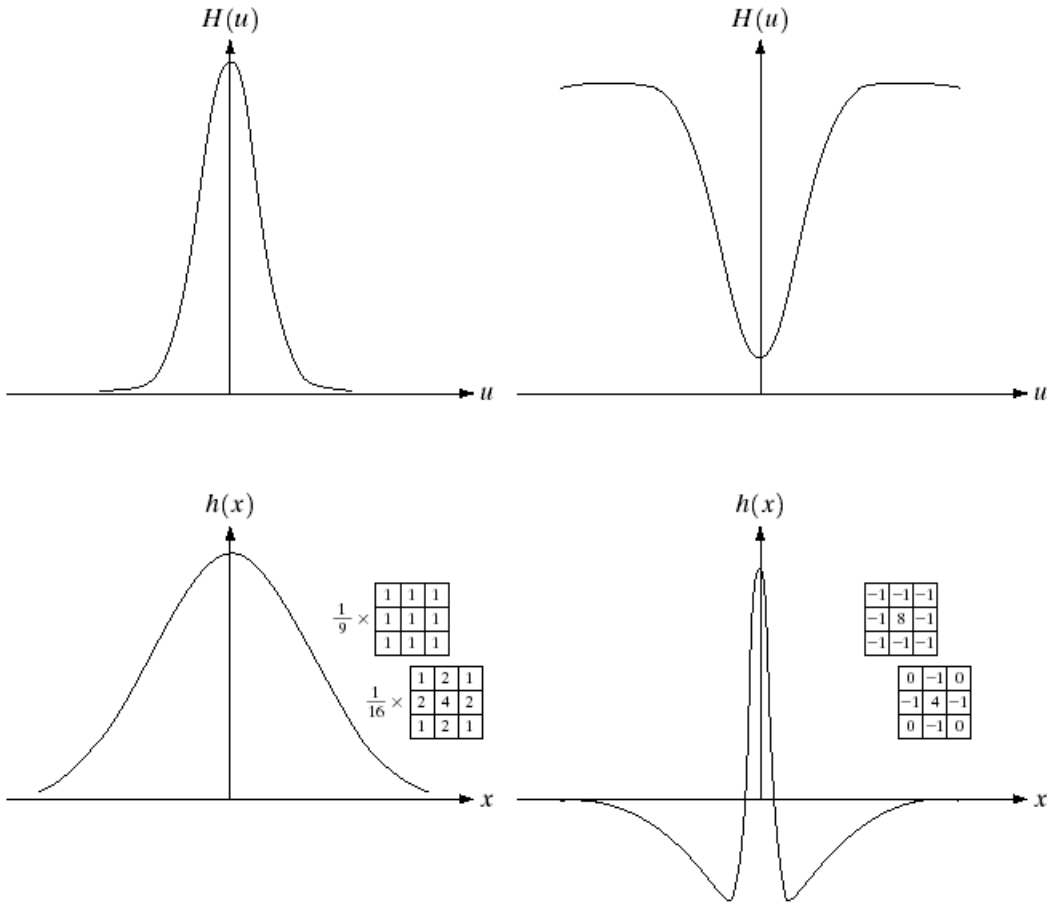

a b
c d

FIGURE 4.9
(a) Gaussian frequency domain lowpass filter.
(b) Gaussian frequency domain highpass filter.
(c) Corresponding lowpass spatial filter.
(d) Corresponding highpass spatial filter. The masks shown are used in Chapter 3 for lowpass and highpass filtering.

Cont.

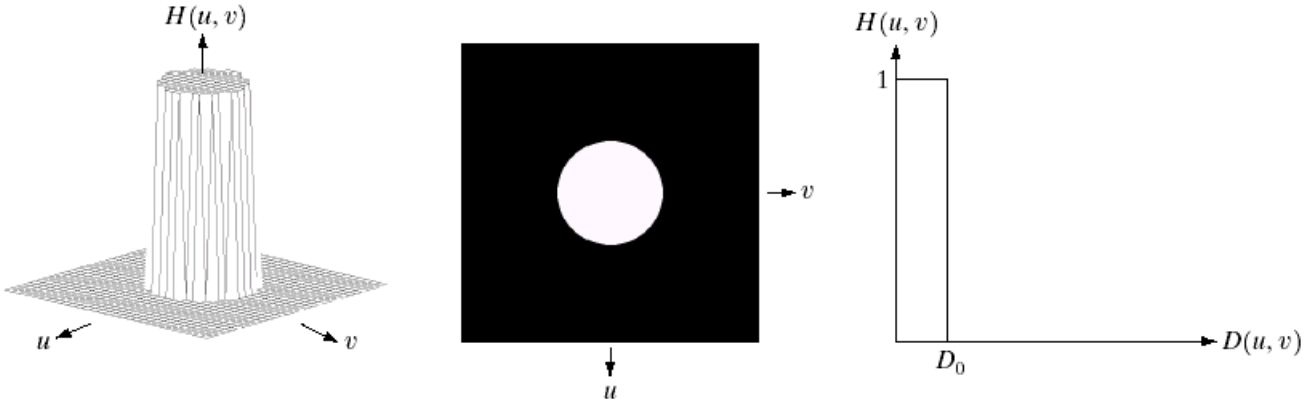

a b c

FIGURE 4.10 (a) Perspective plot of an ideal lowpass filter transfer function. (b) Filter displayed as an image. (c) Filter radial cross section.

Cont.

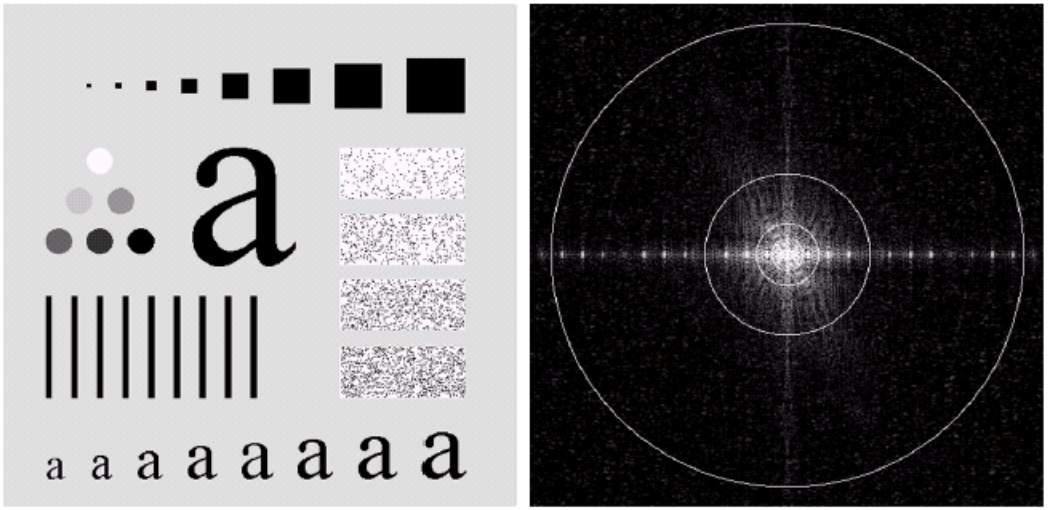

a b

FIGURE 4.11 (a) An image of size 500 × 500 pixels and (b) its Fourier spectrum. The superimposed circles have radii values of 5, 15, 30, 80, and 230, which enclose 92.0, 94.6, 96.4, 98.0, and 99.5% of the image power, respectively.

Cont.

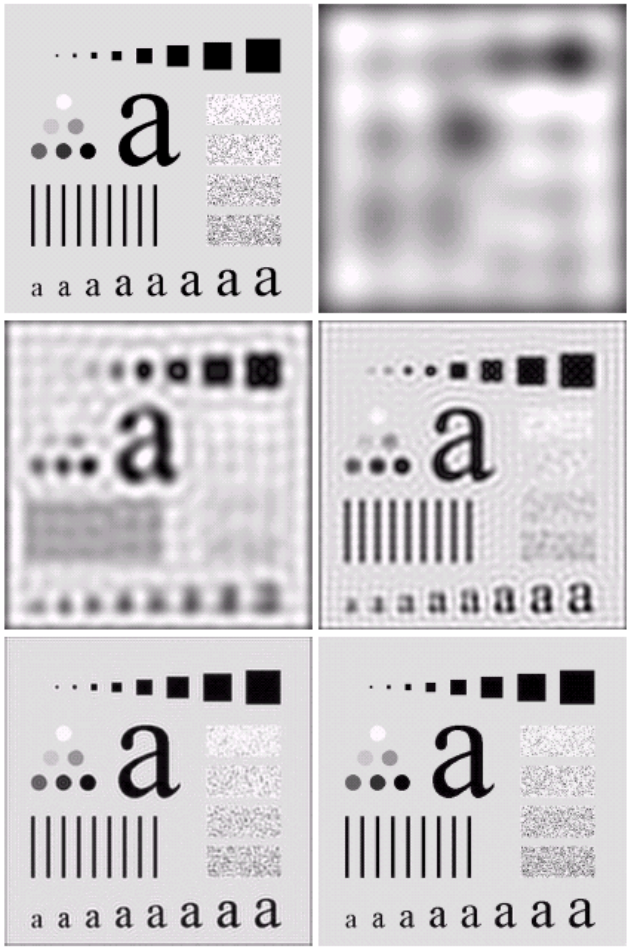

cont

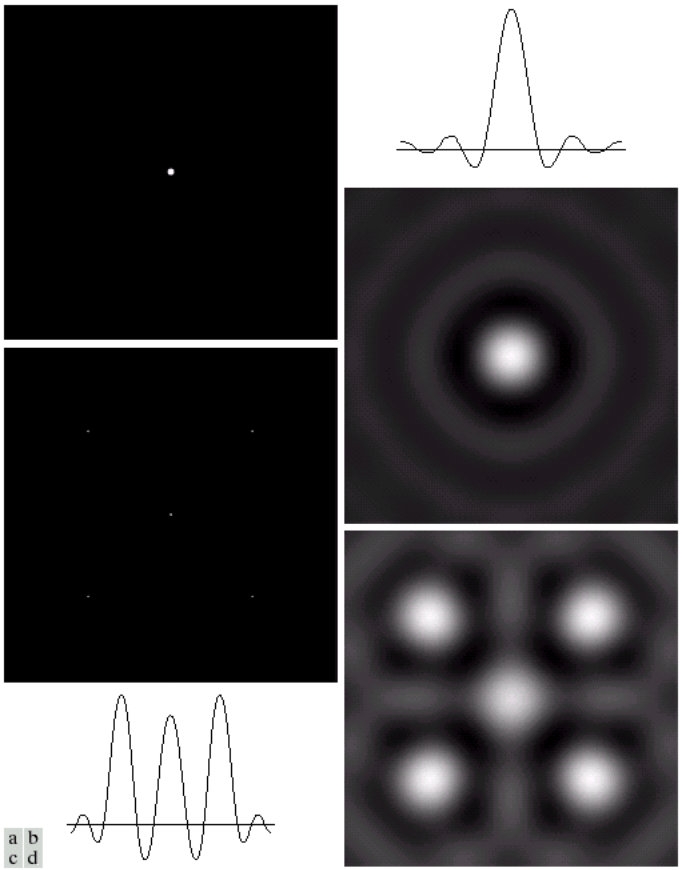

a b
c d

FIGURE 4.13 (a) A frequency-domain ILPF of radius 5. (b) Corresponding spatial filter (note the ringing). (c) Five impulses in the spatial domain, simulating the values of five pixels. (d) Convolution of (b) and (c) in the spatial domain.

cont

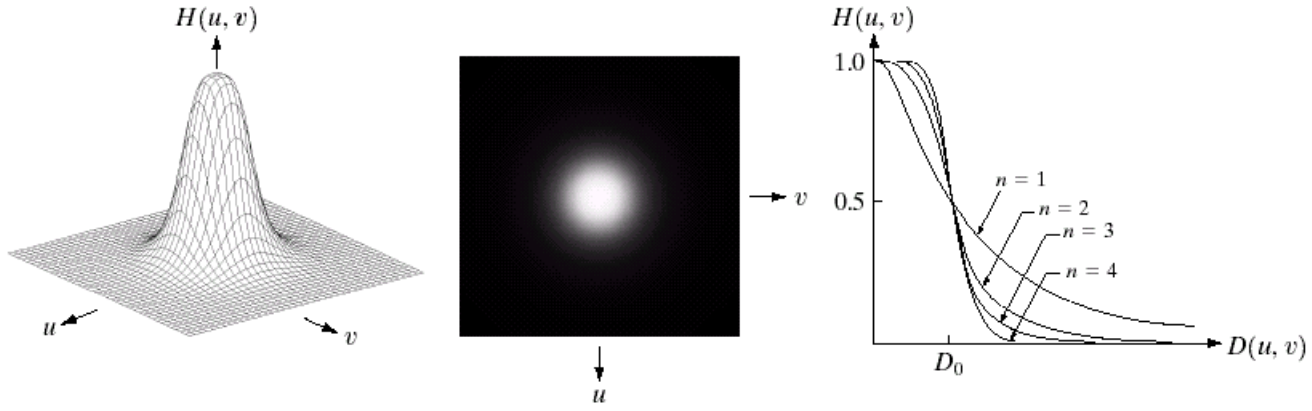

a b c

FIGURE 4.14 (a) Perspective plot of a Butterworth lowpass filter transfer function. (b) Filter displayed as an image. (c) Filter radial cross sections of orders 1 through 4.

Cont.

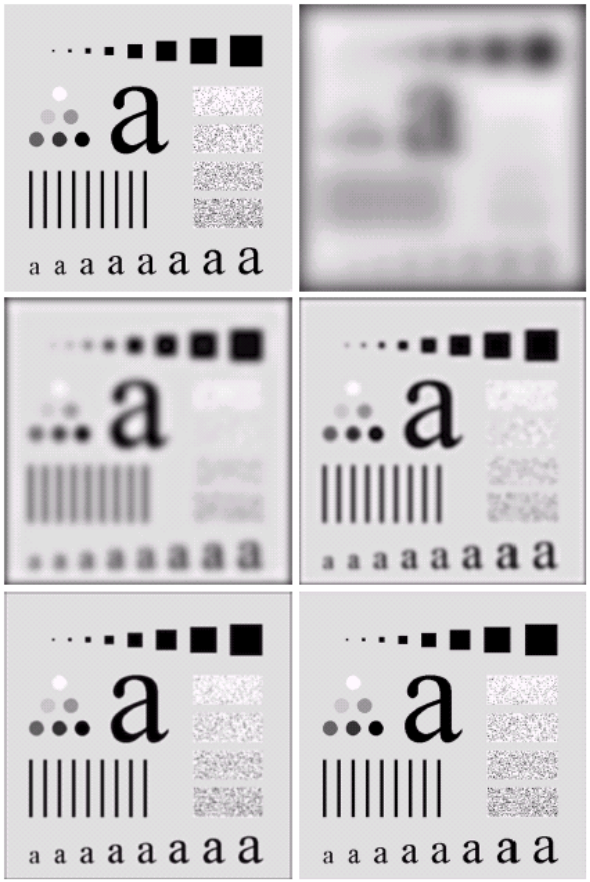

a b
c d
e f

FIGURE 4.15 (a) Original image. (b)–(f) Results of filtering with BLPFs of order 2, with cutoff frequencies at radii of 5, 15, 30, 80, and 230, as shown in Fig. 4.11(b). Compare with Fig. 4.12.

Cont

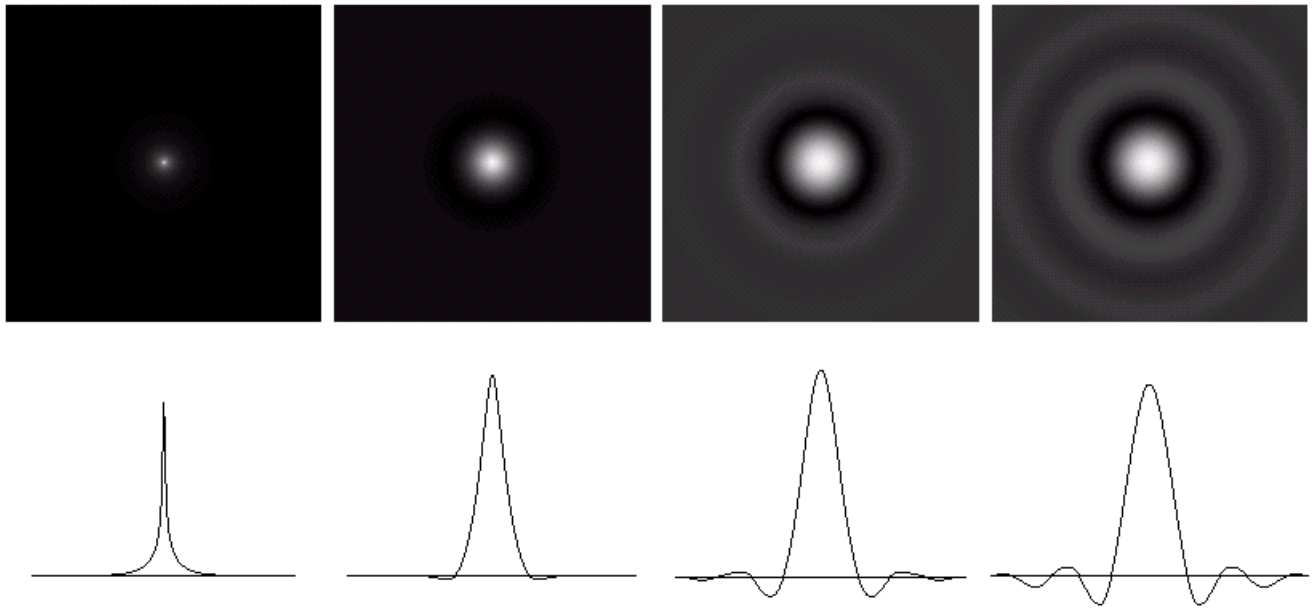

a b c d

FIGURE 4.16 (a)–(d) Spatial representation of BLPFs of order 1, 2, 5, and 20, and corresponding gray-level profiles through the center of the filters (all filters have a cutoff frequency of 5). Note that ringing increases as a function of filter order.

Cont.

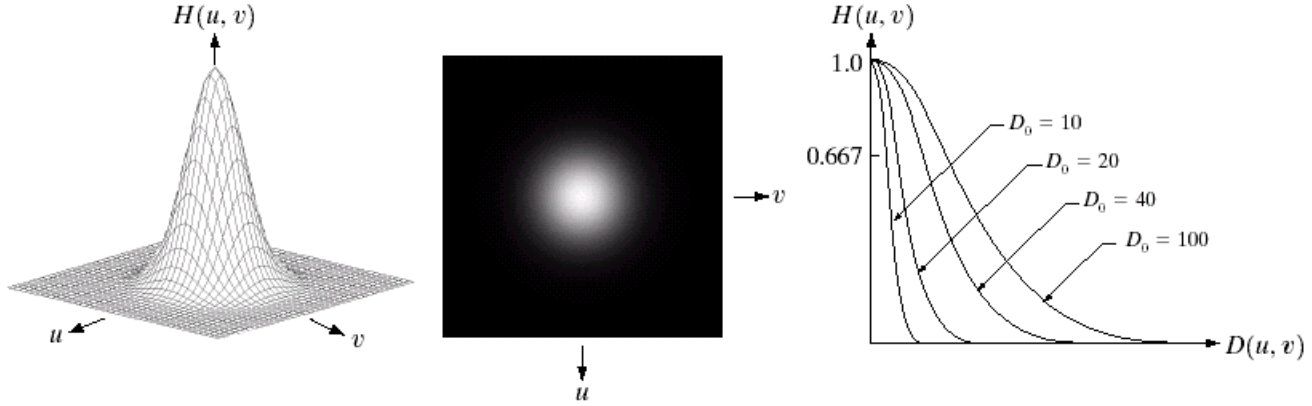

a b c

FIGURE 4.17 (a) Perspective plot of a GLPF transfer function. (b) Filter displayed as an image. (c) Filter radial cross sections for various values of D_0.

Cont.

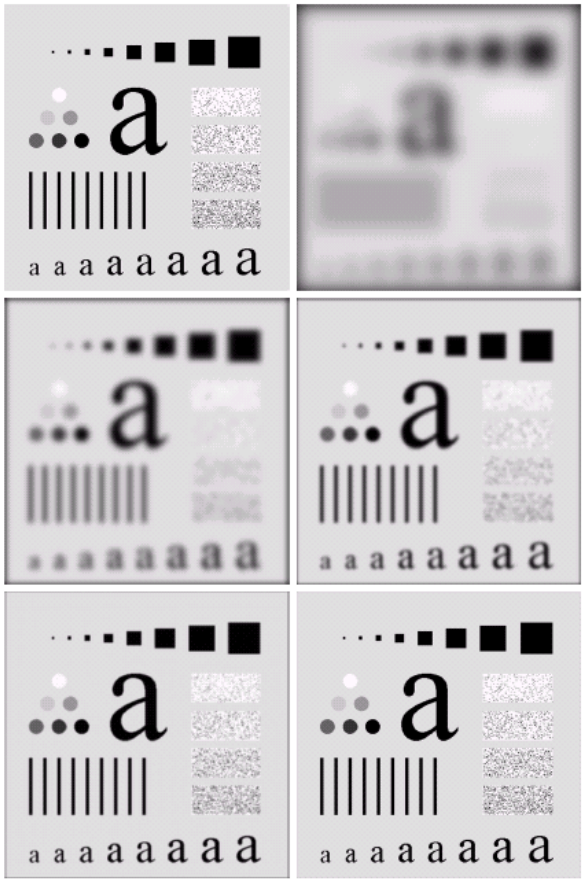

FIGURE 4.18 (a) Original image. (b)–(f) Results of filtering with Gaussian lowpass filters with cutoff frequencies set at radii values of 5, 15, 30, 80, and 230, as shown in Fig. 4.11(b). Compare with Figs. 4.12 and 4.15.

a b
c d
e f

Cont.

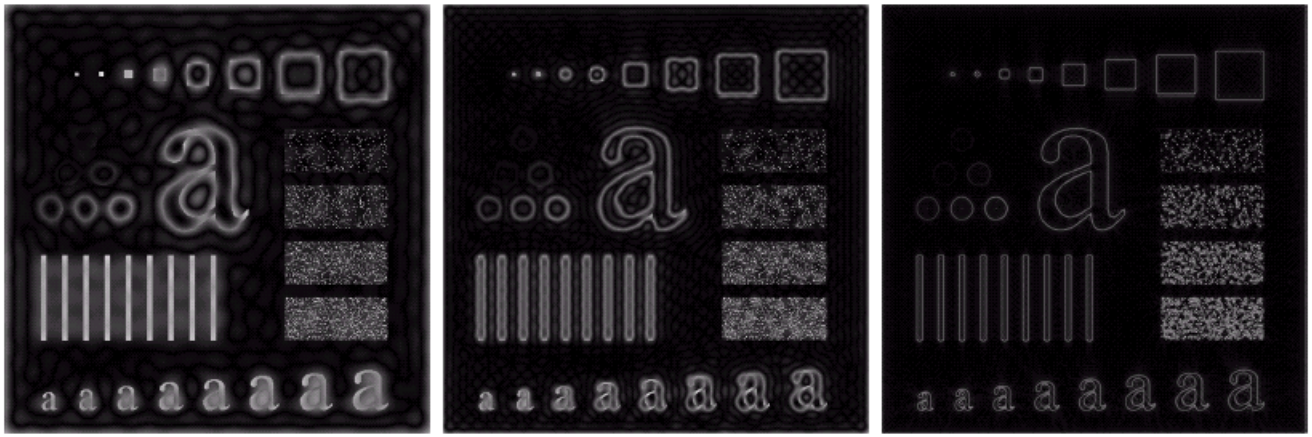

a b c

FIGURE 4.24 Results of ideal highpass filtering the image in Fig. 4.11(a) with $D_0 = 15$, 30, and 80, respectively. Problems with ringing are quite evident in (a) and (b).

Cont.

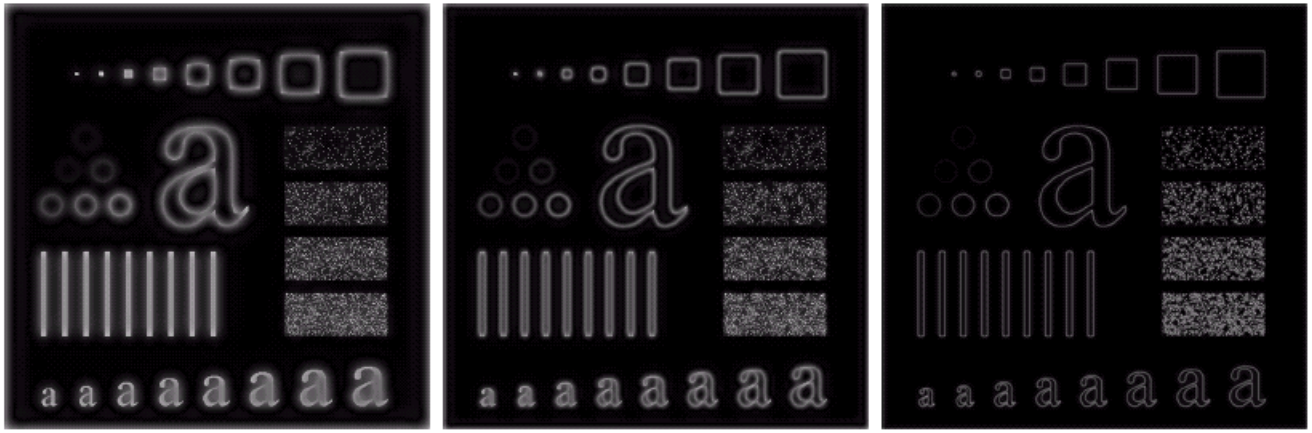

a b c

FIGURE 4.25 Results of highpass filtering the image in Fig. 4.11(a) using a BHPF of order 2 with $D_0 = 15$, 30, and 80, respectively. These results are much smoother than those obtained with an ILPF.

Image enhancement

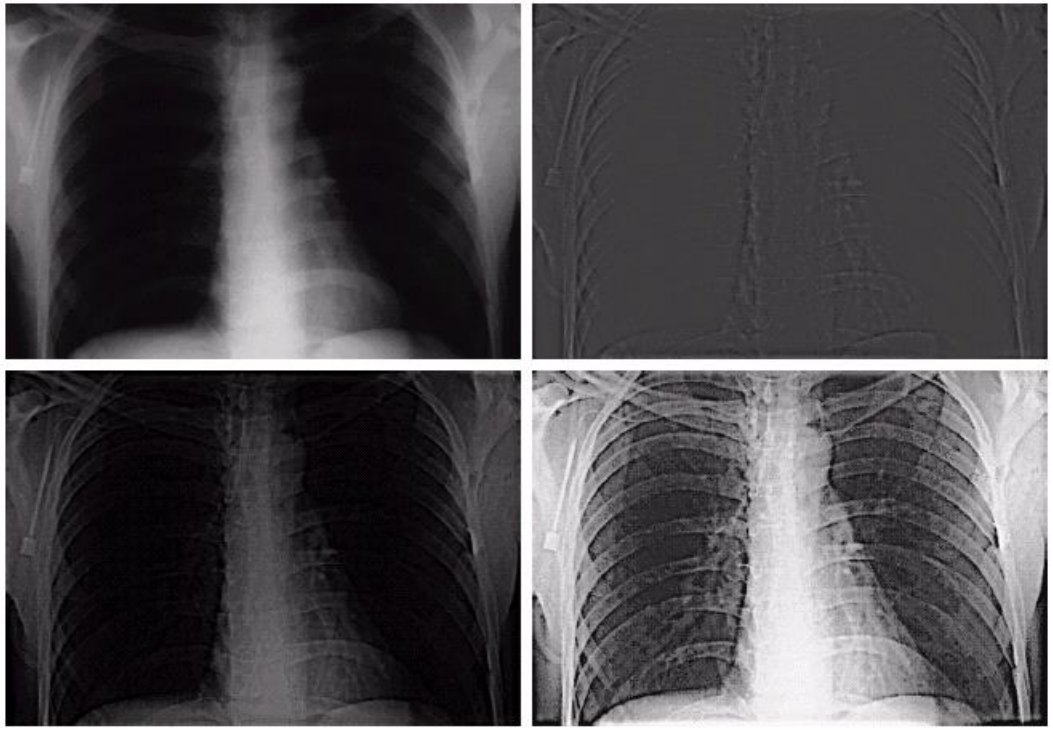

a b
c d

FIGURE 4.30
(a) A chest X-ray image. (b) Result of Butterworth highpass filtering. (c) Result of high-frequency emphasis filtering. (d) Result of performing histogram equalization on (c). (Original image courtesy Dr. Thomas R. Gest, Division of Anatomical Sciences, University of Michigan Medical School.)

a b

FIGURE 4.19
(a) Sample text of poor resolution (note broken characters in magnified view). (b) Result of filtering with a GLPF (broken character segments were joined).

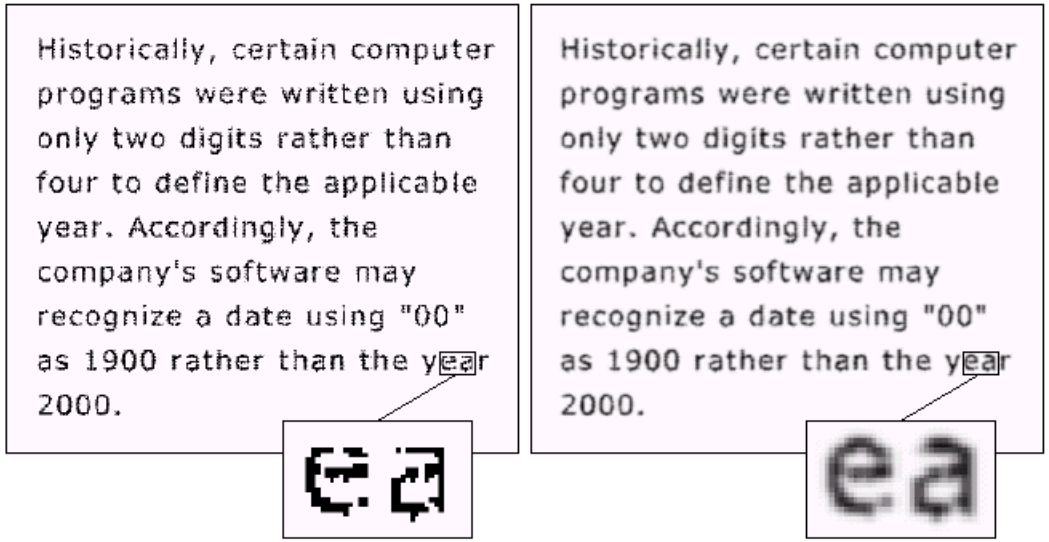

Cont.

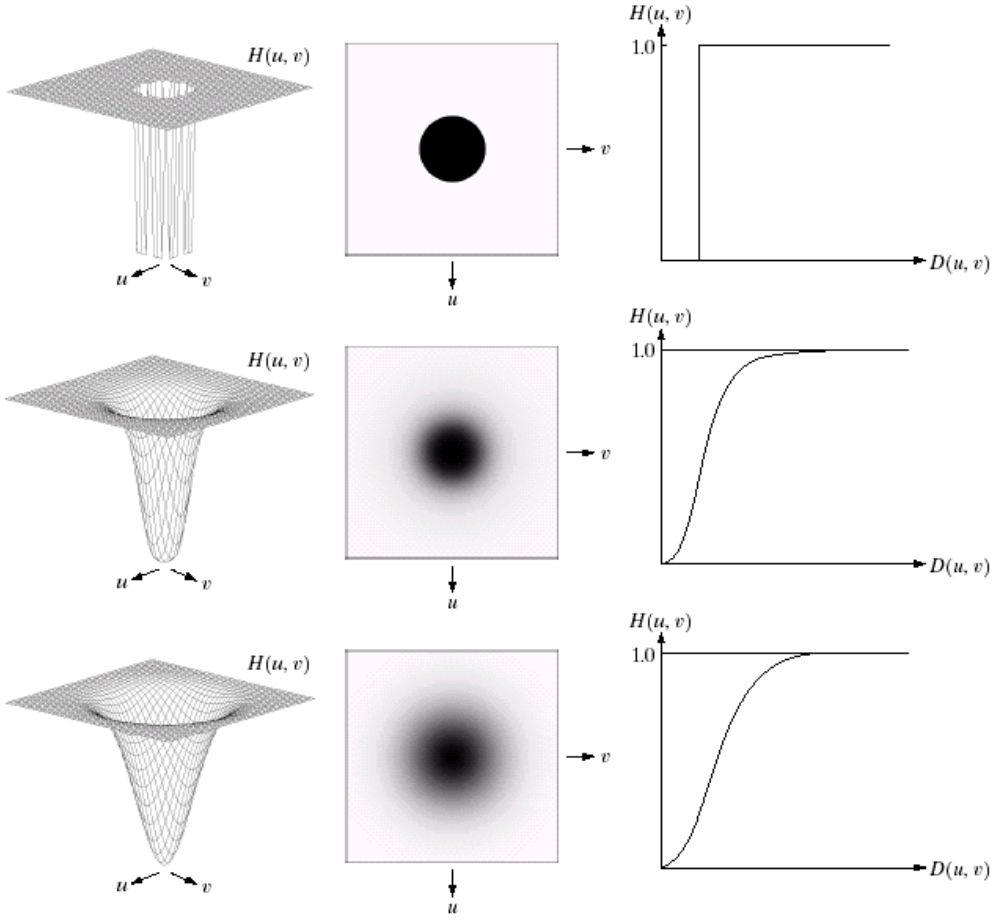

a b c
d e f
g h i

FIGURE 4.22 Top row: Perspective plot, image representation, and cross section of a typical ideal highpass filter. Middle and bottom rows: The same sequence for typical Butterworth and Gaussian highpass filters.

Cont.

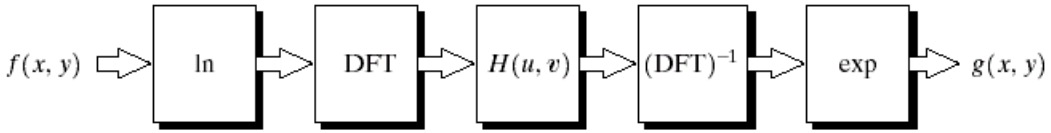

FIGURE 4.31 Homomorphic filtering approach for image enhancement.

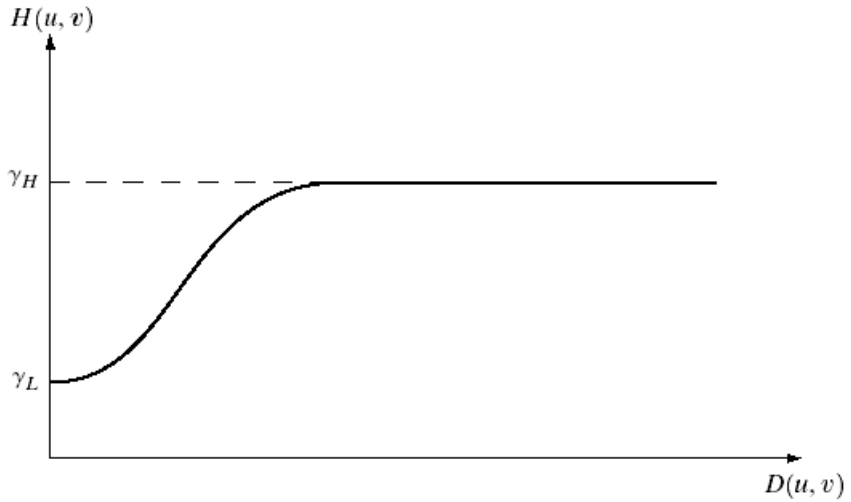

FIGURE 4.32 Cross section of a circularly symmetric filter function. $D(u, v)$ is the distance from the origin of the centered transform.

Cont.

a b

FIGURE 4.33
(a) Original image. (b) Image processed by homomorphic filtering (note details inside shelter). (Stockham.)

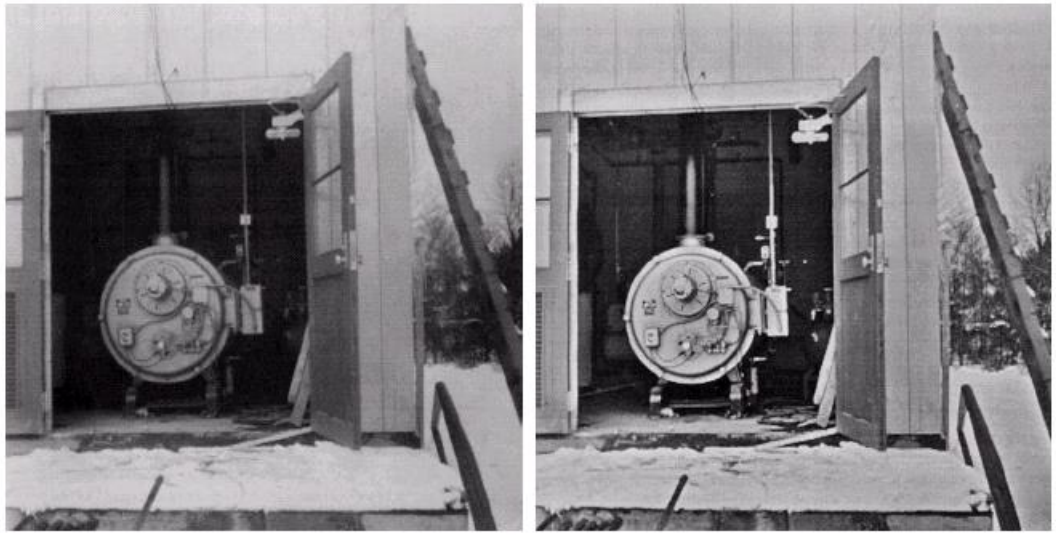

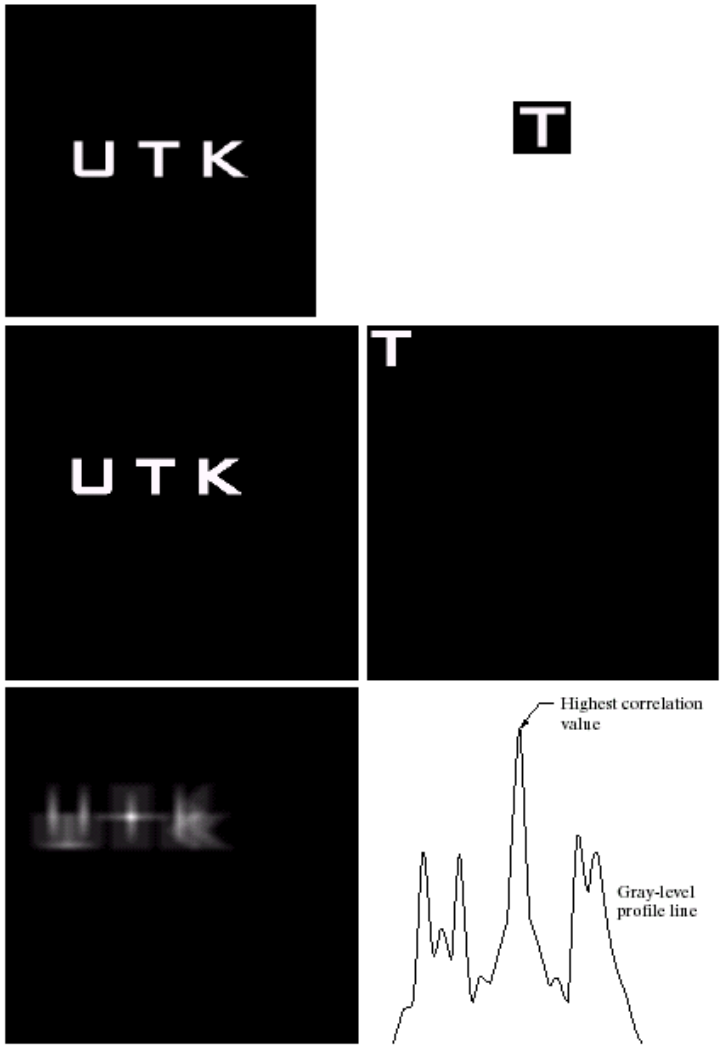

a b
c d
e f

FIGURE 4.41
(a) Image.
(b) Template.
(c) and
(d) Padded images.
(e) Correlation function displayed as an image.
(f) Horizontal profile line through the highest value in (e), showing the point at which the best match took place.

Cont.

TABLE 4.1
Summary of some important properties of the 2-D Fourier transform.

Property	Expression(s)
Fourier transform	$F(u, v) = \frac{1}{MN} \sum_{x=0}^{M-1} \sum_{y=0}^{N-1} f(x, y) e^{-j2\pi(ux/M + vy/N)}$
Inverse Fourier transform	$f(x, y) = \sum_{u=0}^{M-1} \sum_{v=0}^{N-1} F(u, v) e^{j2\pi(ux/M + vy/N)}$
Polar representation	$F(u, v) = \lvert F(u, v) \rvert e^{-j\phi(u,v)}$
Spectrum	$\lvert F(u, v) \rvert = \left[R^2(u, v) + I^2(u, v) \right]^{1/2}$, $R = \text{Real}(F)$ and $I = \text{Imag}(F)$
Phase angle	$\phi(u, v) = \tan^{-1}\left[\frac{I(u, v)}{R(u, v)} \right]$
Power spectrum	$P(u, v) = \lvert F(u, v) \rvert^2$
Average value	$\bar{f}(x, y) = F(0, 0) = \frac{1}{MN} \sum_{x=0}^{M-1} \sum_{y=0}^{N-1} f(x, y)$
Translation	$f(x, y) e^{j2\pi(u_0 x/M + v_0 y/N)} \Leftrightarrow F(u - u_0, v - v_0)$ $f(x - x_0, y - y_0) \Leftrightarrow F(u, v) e^{-j2\pi(ux_0/M + vy_0/N)}$ When $x_0 = u_0 = M/2$ and $y_0 = v_0 = N/2$, then $f(x, y)(-1)^{x+y} \Leftrightarrow F(u - M/2, v - N/2)$ $f(x - M/2, y - N/2) \Leftrightarrow F(u, v)(-1)^{u+v}$

Cont.

Property	Expression(s)
Computation of the inverse Fourier transform using a forward transform algorithm	$\frac{1}{MN} f^*(x, y) = \frac{1}{MN} \sum_{u=0}^{M-1} \sum_{v=0}^{N-1} F^*(u, v) e^{-j2\pi(ux/M + vy/N)}$ This equation indicates that inputting the function $F^*(u, v)$ into an algorithm designed to compute the forward transform (right side of the preceding equation) yields $f^*(x, y)/MN$. Taking the complex conjugate and multiplying this result by MN gives the desired inverse.
Convolution†	$f(x, y) * h(x, y) = \frac{1}{MN} \sum_{m=0}^{M-1} \sum_{n=0}^{N-1} f(m, n) h(x - m, y - n)$
Correlation†	$f(x, y) \circ h(x, y) = \frac{1}{MN} \sum_{m=0}^{M-1} \sum_{n=0}^{N-1} f^*(m, n) h(x + m, y + n)$
Convolution theorem†	$f(x, y) * h(x, y) \Leftrightarrow F(u, v) H(u, v)$; $f(x, y) h(x, y) \Leftrightarrow F(u, v) * H(u, v)$
Correlation theorem†	$f(x, y) \circ h(x, y) \Leftrightarrow F^*(u, v) H(u, v)$; $f^*(x, y) h(x, y) \Leftrightarrow F(u, v) \circ H(u, v)$

Cont.

Some useful FT pairs:

Impulse	$\delta(x, y) \Leftrightarrow 1$
Gaussian	$A\sqrt{2\pi}\sigma e^{-2\pi^2\sigma^2(x^2+y^2)} \Leftrightarrow Ae^{-(u^2+v^2)/2\sigma^2}$
Rectangle	$\text{rect}[a, b] \Leftrightarrow ab\dfrac{\sin(\pi ua)}{(\pi ua)}\dfrac{\sin(\pi vb)}{(\pi vb)}e^{-j\pi(ua+vb)}$
Cosine	$\cos(2\pi u_0 x + 2\pi v_0 y) \Leftrightarrow \dfrac{1}{2}[\delta(u + u_0, v + v_0) + \delta(u - u_0, v - v_0)]$
Sine	$\sin(2\pi u_0 x + 2\pi v_0 y) \Leftrightarrow j\dfrac{1}{2}[\delta(u + u_0, v + v_0) - \delta(u - u_0, v - v_0)]$

† Assumes that functions have been extended by zero padding.